Role of electronic localization and charge-vibrational coupling in resonant photoelectron spectra of polymers: Application to poly(*para*-phenylenevinylene)

R. Friedlein,[1,*] S. L. Sorensen,[2] A. Baev,[3] F. Gel'mukhanov,[3,†] J. Birgerson,[1,‡] A. Crispin,[1] M. P. de Jong,[1] W. Osikowicz,[1] C. Murphy,[4] H. Ågren,[3] and W. R. Salaneck[1]

[1]*Department of Physics (IFM), Linköping University, S-581 83 Linköping, Sweden*
[2]*Department of Synchrotron Radiation Research, Institute of Physics, Lund University, Box 118, S-221 00 Lund, Sweden*
[3]*Theoretical Chemistry, Roslagstullsbacken 15, Royal Institute of Technology, S-106 91 Stockholm, Sweden*
[4]*CDT Ltd., Greenwich House, Madingley Road, Cambridge CB3 0HJ, United Kingdom*
(Received 5 September 2003; published 9 March 2004)

A combination of x-ray absorption and resonant photoemission (RPE) spectroscopy has been used to study the electronic structure of the one-dimensional conjugated polymer poly(*para*-phenylenevinylene) in nonordered (as prepared) thin films. The dispersion of RPE features for the decay to localized and delocalized bands are qualitatively different. A theory for band dispersion of RPE in polymers is given, showing the important roles of electronic state localization and vibrational (phonon) excitations for the character of the dispersion.

I. INTRODUCTION

Conjugated, semiconducting, organic polymers have evolved from the world of electrically conducting polymers (Nobel prize in Chemistry, 2000), through field-effect transistors[1,2] and light-emitting devices,[3] to emerging applications in plastic electronics and flat panel display systems. The efficient implementation of these materials in applications requires a detailed understanding of the electronic and optoelectronic processes underlaying the function of devices. In this context, conjugated polymers are characterized by specific comprehensive properties which cannot be matched by other materials.

(i) A polymer chain represents a (quasi-) one-dimensional electronic system. Its spatial extension is in between that of smaller molecules and extended higher-dimensional solids. Results obtained for individual polymer chains and bulk material constitute a link between these two limiting cases, eventually allowing the relatively detailed picture of electronic phenomena in smaller systems to be transferred to more comples ones.

(ii) The one-dimensionality is responsible for a high structural flexibility which leads to strong charge-phonon coupling and therefore to significant vibrational relaxation phenomena.[4]

(iii) Due to the high polarizability of organic π-systems intra- and intermolecular screening of charge carriers and electronic excitations is substantial.[5,6]

(iv) As compared to smaller molecules, Coulomb interactions between charges in delocalized states are rather week. These interactions increase with the degree of localization.[7,8]

Specific information regarding these properties can be obtained using high-energy spectroscopic techniques.[9–12] For example, the dynamic response of the interrogated system to the sudden and vertical photoionization can be studied by Ultraviolet- (UPS) and x-ray (XPS) photoelectron spectroscopy.[4,9,13] Energy-loss of high-energy electrons as measured in electron-energy loss spectroscopy in transmission provides the momentum dependence of (low energy)

collective electronic excitations.[10–12] Information on the electronic screening response following an excitation of a core-electron into bound unoccupied states is inhibited in near-edge x-ray absorption (NEXAFS) spectra.[14] More information can be obtained by studying the decay of this excited state. This decay occurs *via* several processes:[15–17] radiative x-ray emission or nonradiative decay through (i) normal Auger electron emission, (ii) participator Auger decay, and (iii) spectator Auger decay (Fig. 1). The latter leads to a two-hole one-particle final state while the former populates one-hole final states,[16] and might therefore also be called resonant photoemission, RPE. The participator Auger scattering is, however, not vertical in nature, possibly leading to the occupation of *different vibrational* sublevels of the given electronic final state, depending on the excitation energy $\hbar\omega$. The kinetic energy of the emitted electron can either disperse linearly with ω (Raman dispersion) or it can be constant.[18] In the general case the dispersion is nonlinear.[19–21] There are different possible reasons for such a nonlinearity: conservation of electronic momentum as in radiative x-ray scattering from periodic systems,[19,22] broadenings originating in the spectral function of the incident radiation,[23–25] a specific vibrational structure in the core-excited and final states,[20] quenching[26] and dephasing[27] of transitions, and charge transfer to systems in contact.[28,29]

The physics related to the dispersion of RPE final states is well studied for atoms and relatively small molecules (with less than about 10 atoms),[17] while for solids and large molecules the situation remains basically unexplored, probably due to the complexity of the issue for such systems. Such, RPE spectroscopy has only rarely been used to study organic and purely-carbon-based solid materials. Among the few exceptions are graphite,[30] C_{60},[15,31] polystyrene,[32] and pure as well as nitrogen-substituted benzene.[16,33] Difficulties in the interpretation of the decay spectra arise from the combination of the nature of the intermediate core-excited state as the initial state for the decay process, the character of the Coulomb matrix elements, and the role of vibrational excitations in the intermediate core-excited and RPE final states.

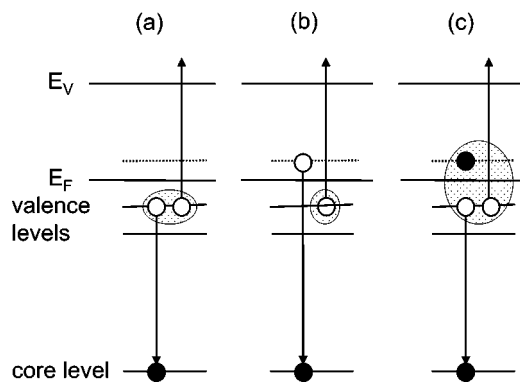The resonant Auger scattering processes in poly-(*para*-

FIG. 1. Nonradiative core-hole decay processes: (a) normal Auger decay (nonresonant), (b) participator, and (c) spectator decay following the resonant core excitation. Final-state configurations are marked by dotted areas. The Fermi level and the vacuum level are denoted E_F and E_V, respectively.

phenylenevinylene) (PPV) molecules, with the chemical structure shown in Fig. 2, might still be relatively simple cases of resonant nonradiative decay processes in extended electronic systems. Depending on the character of the unoccupied bands populated in the intermediate state, these core-excited states can be either strongly localized or delocalized. The role of the degree of electronic localization on the nonradiative decay processes can be investigated in terms of the momentum dependence of the electronic (Coulomb) interaction and of the role of vibrational degrees of freedom in the deexcitation process. An interpretation of these processes should be based on an interplay between vibrational broadening and the dispersion of electronic bands, and on the dependence of the Auger matrix elements on the electron wave number in the solid.

The paper is organized as follows. After the description of the PPV material used and of conditions under which the experiment was performed (Sec. II), a first analysis of the experimental results is given in Sec. III. Next, the theoretical model of the participator Auger scattering is described in Sec. IV: Conservation of the electron momentum is investigated in Part A, while in Part B it is shown how the vibrational degrees of freedom can influence the dispersion of the resonant features. Secs. V and VI are devoted to the numerical calculation of resonant decay spectra of PPV and to the discussion of their properties. The results are summarized in Sec. VII.

II. EXPERIMENT

The PPV samples were made by conversion of spin-coated films of the sulphonium precursors,[34] on clean gold substrates, as described elsewhere.[35] This procedure provides homogeneous films over a large (~ 1 cm^2) area.[36] Measured valence-band photoelectron emission spectra at different spots were virtually indistinguishable from each other. The films were sufficiently thick (~ 20 nm) to suppress the features from the substrate, but were still thin enough to avoid charging. The defect density in the converted material has been determined by (Infrared-) Raman spectroscopy to be
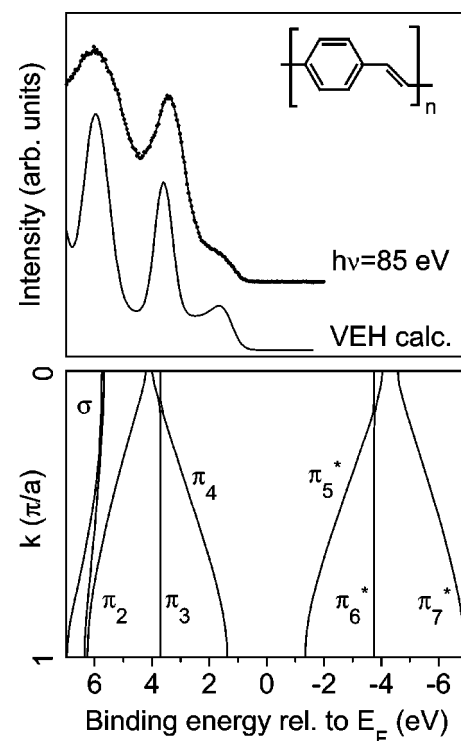

FIG. 2. The band structure (lower panel) of PPV calculated using the valence effective Hamiltonian (VEH) method, rescaled and replotted from Ref. 36, and the resulting broadened DOS in comparison with the valence-band spectrum obtained with 85-eV photons.

about 5%. Statistically, each conjugated chain segment contains an average of about 20 to 25 repeat units. It is worth pointing out that many earlier electron spectroscopic studies have probably been performed on material with substantially shorter conjugation lengths. PPV is known to be stable in air, at room temperature, and in the dark.[37] Physisorbed water molecules can be easily removed by heating in UHV at temperatures above 400 K.[37]

The spectra were obtained at the electron storage ring MAX-Lab in Lund, Sweden. The NEXAFS and RPE measurements were carried out at the beam lines I411 and I311, respectively, at MAX-II.[38] The NEXAFS spectra were recorded in 50-meV photon energy steps with the Auger yield technique using the Scienta SES-200 electron energy analyzer of beam line I411. The C KLL Auger electrons were collected with a kinetic-energy window between 260 and 274 eV. The data were normalized using the spectrum of a freshly sputtered gold sample. The NEXAFS spectra were identical for all angles between the electric-field vector of the incident light and the sample surface normal, indicating that, other than a possible partial preferential orientation parallel to the substrate surface, the spin-coated samples were not ordered on a macroscopic scale. The RPE spectra were taken with the Scienta SES-200 electron energy analyzer of beam line I311, the energy resolution set to 60 meV. The spectral width of the incident radiation was matched with the energy resolution of the electrons. The long-term beam stability was within 50 meV, as measured by the position of the C(1s) line excited by second-order light. Recording of this line simul-

taneously with the decay spectra provided the determination of the exact photon energy and the alignment of the spectra on the binding-energy scale. The intensities of the spectra were normalized to absolute values of the photon flux. Absolute intensities of spectra measured at different spots were normalized using the C($1s$) intensities. To avoid any possible degradation of the polymer samples during the long exposure to high-energy photons during the RPE measurements, the irradiated spot on the sample was moved systematically. No beam damage effects were observed in the valence band spectra obtained with 85-eV photons.

III. EXPERIMENTAL RESULTS AND DISCUSSION

The lowest binding energy portion of the calculated one-dimensional (1D) electronic band structure of poly(*para*-phenylenevinylene), or PPV, is shown in Fig. 2 (adapted from Ref. 36). The frontier (delocalized) π and $\pi^\star$ bands are derived from the outermost doubly degenerate $1e_{1g}$ orbital of the benzene molecule.[36] One of these two bands, labeled π_3, is localized on the carbon atoms in the *ortho*positions, those which are not bound to the vinylene group, while the wave function of the other has a strong overlap with the π state of the vinylene group, leading to the strongly dispersed (delocalized) π_4 band.[36,39] The calculated band structure is very symmetrical, that is, the unoccupied π bands mirror the occupied $\pi^\star$ bands. The π_3 and π_4 bands intersect close to $k=0$, center of the 1D Brillouin zone,[36] which reaches from $k=-\pi/a$ to π/a. The volume of the first Brillouin zone is $\tau=2\pi/a$. At the zone edges and in the center of the Brillouin zone at $k=0$, the dispersed bands should lead to characteristic van-Hove singularities in the density of states (DOS), as in all 1D systems. This is seen for PPV in UPS spectra,[36,40] as well as in the spectrum obtained with 85-eV photons (Fig. 2).

In Fig. 3(a) the NEXAFS spectrum of PPV is shown. In the presence of the core hole, the spectrum is excitonic. The onset at about 283.9 eV is about 1 eV below the C($1s$) core level binding energy of 284.9 eV. In the region up to about 6 eV above threshold, the NEXAFS spectrum exhibits three main features, at approximately 285, 287.5, and 289 eV, all of which are resonances with $\pi^\star$-final state symmetry.[10] At higher energies, the features correspond to states with $\sigma^\star$ symmetry.[10] In the present spectrum, new fine structure is observed in the first resonance region above the core-excitation threshold, between 284.1 eV and about 285.8 eV, which was not seen in previous studies of thick films of PPV,[10,41] nor even in monolayers of PPV on surfaces of molydenium disulfide.[42] In the present highly resolved spectrum, in addition to the sharp peak at 284.9 eV, three shoulders are seen, two on the low-energy and one at the high-energy side.

In order to understand the origin of these features, the decay of the core-excited state, and especially the participator Auger scattering channels might be studied. The participator decay of a resonant core-hole excited-state in a molecular solid is a major contribution to resonant spectra as long as intra-molecular core-hole screening is dominant, and as long as the excited electron is localized on the molecule
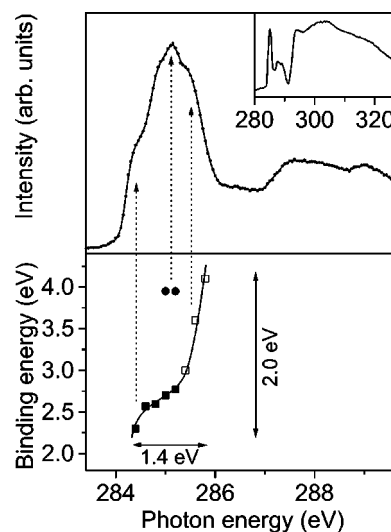

FIG. 3. (a) NEXAFS spectrum of PPV in a narrow and wider (inset) energy range. (b) The position of the RPE peaks related to the the π_3 and π_4 bands as a function of the photon energy. The nondispersing features at highest intensity is marked by full circles. The dispersing π_3- band leads to the mapping of the $\pi_5^\star$-band in the presence of a core hole (full and open squares). Full squares indicate visible peak positions, open squares represent approximate values. Furthermore, the width of the π_3 and of the distorted $\pi_5^\star$ band are indicated.

probed.[15] Such RPE events are easily identified as sharp features with strongly varying intensities as a function of the photon energy.[15] In addition to resonant features, at any photon energy, the usual valence band photoelectron emission occurs. The intensity, however, due to the competing x-ray absorption processes, should be suppressed in the vicinity of the core-hole excitation energy, and does not usually exceed the intensity of the spectrum below threshold.

In Fig. 4, the RPE spectra in the energy region near threshold, taken with photon energy steps of 0.2 eV, are shown. In addition to the broad, unstructured background, which stems from normal Auger and spectator processes, a resonant enhancement of all structures between about 2 and at least 13 eV can be seen, as the photon energy is tuned to the C($1s$)-$\pi^\star$ resonances. The resonant behavior vanishes for photon energies above about 286 eV, where ionization processes start to occur. However, the resonant enhancement of the two structures at lowest binding energy is by far strongest. According to the normal (nonresonant) valence-band spectrum, the two strong features correspond to electrons in the π-bands of PPV. First, the nondispersing peak at about 3.85-eV binding energy, which is related to the localized π_3 state, appears at a photon energy of about 284.8 eV, that is, in the middle of the NEXAFS resonance. A very similar feature has been observed for polystyrene as the single dominating π feature.[32] This peak arises from states localized on the phenylene group. For PPV, a second, strongly dispersing feature starts to appear at a threshold energy of $\hbar\omega$ = 284.2 eV, on the low binding-energy side of the spectrum. This structure is related to the π_4 band. At energies around $\hbar\omega$ = 284.4 eV, the spectral weight of this peak is high because of the van-Hove singularity in the DOS at the edge of
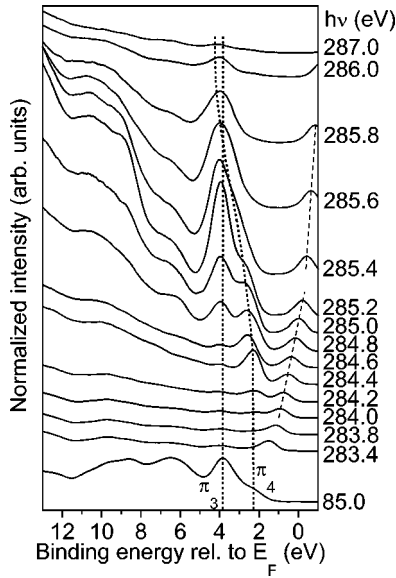
FIG. 4. RPE spectra for photon energies in the vicinity of the the C($1s$) core level threshold and at a photon energy of 85 eV. The position of the C($1s$) line excited by second-order light is indicated by a dashed line.

FIG. 5. Scheme of the participator Auger scattering process depicted in Eq. (1). θ is the angle between the momentum of the Auger electron **q** and the chain axis.

the band. For higher photon energies, the peak disperses to higher binding energies, and merges with the nondispersing π_3-derived peak.

At the onset of the resonance at $\hbar\omega=284.2$ eV, RPE emission occurs only from a small part of the delocalized band, and is thus sensitive to a distinct part of the Brillouin zone. It needs to be investigated if by changing the photon energy, different parts of the 1D Brillouin zone are accessed. Considering the ground-state band structure of PPV, the observed behavior might indicate the existence of a dispersed but distorted $\pi_5^\star$ band in the core-hole excited state. Returning to the NEXAFS spectrum of Fig. 3(a), the fine structure in the first resonance might be understood. Plotting the RPE peak positions versus the photon energy, as in Fig. 3(b), the dispersion in the final states can be correlated to the positions of the peaks in the NEXAFS spectrum, as indicated in Fig. 3(b). While the sharp peak of the NEXAFS resonance corresponds to C($1s$)-to-$\pi_6^\star$ transitions, the lowermost and uppermost shoulders on the low- and high-binding energy sides are related to the (core-hole-distorted) $\pi_5^\star$-band. From Fig. 3(b) the width of this band is only 1.4 ± 0.2 eV. It is significantly smaller than that of the ground-state π_4 band, for which a width of 2.0 ± 0.2 eV is measured. Furthermore, the (distorted) $\pi_6^\star$-band is pulled down to almost the middle of the $\pi_5^\star$-band, about 0.6 to 0.7 eV from the upper $\pi_6^\star$-band edge. Such a behavior is expected if one of the two bands is more localized than the other, since screening in localized states should be less than in delocalized states. In contrast to the ground-state band structure, the crossing of the two distorted bands does not occur close to $k=0$ anymore. The third, less pronounced shoulder in the NEXAFS spectrum, close to the sharp peak in the middle of the resonance, does not have a corresponding feature in the RPE spectra. It might therefore be caused by other than participator-type decay
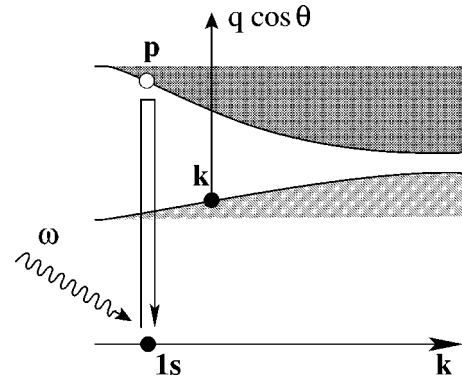
processes which cannot be treated within this paper.

In order to be able to relate spectral features in the NEXAFS spectrum to specific electronic states, the core excitation at chemically different atomic sites into the same part of an unoccupied band must occur at a similar photon energy. This requires a negligible chemical shift in the core level binding energy for the different atomic sites. For PPV, the full width at half maximum of the C($1s$) peak of 0.8 eV is relatively small, and, to a large extent, given by the lifetime of the core-hole state, vibrational broadening as well as variations in the intermolecular polarization energy in a varying local arrangement of the individual polymer chains. Thus, it can be anticipated that chemical shifts of core-level binding energies for the various carbon-atom sites α are small. They will be neglected in the forthcoming discussion, that is, E_{1s}^α is set equal to E_{1s}.

IV. THEORY

The PPV molecule has the character of a 1D chain, for which a core hole can be created in atoms from different unit cells. With an average number N of about 20 unit cells the conjugated segments in the material studied are relatively long. A good approximation is an ideal infinite chain, and continuum quasimomenta can be implemented for the unoccupied (p) and for the occupied (k) valence bands. The wave functions and energies in these bands are denoted (ψ_{vp}, E_{vp}) and (ψ_{ik}, E_{ik}), respectively. The infinite chain model has following two obvious advantages: there are no end effects, and the Bloch theorem is valid.

We explore the participator Auger scattering

$$\omega + |\text{ground}\rangle \Rightarrow |1s_\alpha \rightarrow \psi_{vp}\rangle \Rightarrow |\psi_{vp} \rightarrow 1s_\alpha ; \psi_{ik} \rightarrow \psi_\mathbf{q}\rangle \quad (1)$$

schematically shown in Fig. 5. The core-excited carbon atom is labeled α. The ejection of the Auger electron with the momentum **q** and the energy $E=q^2/2$ (atomic units are used) is characterized by the RPE cross section:[19]

$$\sigma(E,\omega) = \frac{N}{\tau} \int_0^{\pi/a} dk \sum_n |F_n|^2 \delta(\omega - E - (\epsilon_n - \epsilon_0) + E_{ik}).$$

$$(2)$$

Because of the near zero natural lifetime broadening of the final states only the core-excited state width is considered here. The argument of the δ-function reflects the energy conservation law for the overall RPE process. The measured spectra display resonances which are rather broad as compared to the spectral width of the incident radiation. This allows the x-ray beam to be considered as essentially monochromatic of frequency ω.

The scattering amplitude is given by the Kramers-Heisenberg (KH) formula[19] and can be written in the Born-Oppenheimer approximation as

$$F_n = \frac{N}{\tau} \int_0^{\pi/a} dp \sum_{\alpha,m} \frac{\langle n|m\rangle \langle m|0\rangle Q(\mathbf{q}k|p1s_\alpha)D_{\nu p}}{\omega - (E_{\nu p} - E_{1s}) - (\epsilon_m - \epsilon_0) + \iota\Gamma}, \tag{3}$$

where $\langle m|0\rangle$ and $\langle n|m\rangle$ are the many-mode Franck-Condon (FC) amplitudes of the photoabsorption and decay transitions. The FC factors refer to the vibrational part of the scattering process. The quantum numbers and vibrational energies of the ground, core-excited and final states are $(0, \epsilon_0)$, (m, ϵ_m), and (n, ϵ_n), respectively. The electronic matrix elements of photoabsorption and decay read

$$D_{\nu p} = \langle \psi_{\nu p}|\mathbf{e}\cdot\mathbf{d}|1s_\alpha\rangle,$$

$$Q(\mathbf{q}k|p1s_\alpha) = 2[\psi_\mathbf{q}\psi_{ik}|1s_\alpha\psi_{\nu p}] - [\psi_\mathbf{q}\psi_{\nu p}|1s_\alpha\psi_{ik}], \tag{4}$$

respectively, where $\mathbf{e}$ is the polarization vector of the photon, $\mathbf{d}$ is the dipole moment for photoabsorption at frequency ω, and

$$[\psi_i\psi_j|\psi_k\psi_l] = \int d\mathbf{r}_1 \int d\mathbf{r}_2 \psi_i^*(\mathbf{r}_1)\psi_j(\mathbf{r}_1)\frac{1}{r_{12}}\psi_k^*(\mathbf{r}_2)\psi_l(\mathbf{r}_2) \tag{5}$$

the Coulomb integral determining the electronic interaction in the nonradiative participator decay process.

Based on this formalism we can identify two qualitatively different mechanisms which could be responsible for the unusual dispersion seen in PPV RPE spectra. One mechanism is simply conservation of electron momentum in the decay process.[23] The second is related to unresolved excitation processes within the polymer where energy can be stored in vibrational degrees of freedom.[20]

A. Conservation of electron momentum

At first glance the non-Raman dispersion of final state intensities in the participator Auger scattering process (1) for the bands $i = \pi_4$ and $\nu = \pi_5^*$ might be related to momentum conservation of the participating electrons: $k = p$. Such a law might be invoked to explain the strong photon-energy sensitivity of the RPE emission from different parts of the delocalized valence band.

We consider an idealized situation where the π_5^* band is a mirror reflection of the π_4 band. This mimics the band structure depicted in Fig. 2. In this case the sum of E_{ik} and $E_{\nu k}$ is constant and does not depend on k. The peak positions of the RPE spectral features should then be independent of ω. That is, in a purely electronic process, the momentum of the

ejected (Auger) electron k is expected to be independent from the momentum of the core-excited electron p. This motivates a detailed investigation of momentum conservation in the participator RPE process, Eq. (1).

The electronic wave functions $\psi_{\nu p}$ of the unoccupied electronic states are expanded in linear combinations of molecular orbitals χ_ν^β of the unit cell β:

$$\psi_{\nu p} = \frac{1}{\sqrt{N}} \sum_{\beta=1}^N \chi_\nu^\beta e^{\iota p \beta a},$$

$$\chi_\nu^\beta = \chi_\nu(\mathbf{r} - \mathbf{R}_\beta) = \sum_{\delta=1}^K a_{\nu\delta}(p)\phi_\delta. \tag{6}$$

Here, K is the number of carbon atoms in the unit cell, $\mathbf{R}_\beta$ the radius vector of the center of the unit cell β.[43] In general, the coefficients $a_{\nu\delta}(p)$ depend on the momentum of the core-excited electron p. In this study only π bands are of interest. Therefore, ϕ_δ is simply the $2p_\pi(\mathbf{r} - \mathbf{R}_\delta)$ atomic orbital of the carbon atom δ.

In the tight-binding approximation, only the interaction between neighboring cells is accounted for which results in the Hückel solution for the energy of delocalized bands

$$E_{\nu p} = \varepsilon_\nu - \kappa_\nu \cos pa. \tag{7}$$

Expressions similar to those in Eqs. (6) and (7) are valid for occupied states if νp is substituted for ik. The Hückel parameters $\varepsilon_\nu = \langle\chi_\nu|H|\chi_\nu\rangle$ and $\kappa_\nu = \langle\chi_\nu|H|\chi_{\nu\pm1}\rangle$ depend in general on the electron momentum p.

Inserting Eq. (7) into the formula for the scattering amplitude, Eq. (3), leads to

$$F_k = \frac{1}{\tau}NY(\mathbf{e}\cdot\mathbf{d})\mathcal{F}_k,$$

$$\mathcal{F}_k = \int_0^{\pi/a} dp \sum_m \frac{\langle n|m\rangle\langle m|0\rangle\tilde{Q}}{\omega - (E_{\nu p} - E_{1s}) - (\epsilon_m - \epsilon_0) + \iota\Gamma}. \tag{8}$$

Here $\mathbf{d} = \langle\phi|\mathbf{r}|1s\rangle$. The coordinate of the carbon atom δ relative to the center of the unit cell β is denoted $\mathbf{R}_{\delta\beta} = \mathbf{R}_\delta - \mathbf{R}_\beta$. The scattering amplitude depends on the electronic matrix element of the decay

$$\tilde{Q} = [\phi_\mathbf{q}\phi|1s\phi]\sum_{\delta=1}^K a_{i\delta}(k)a_{\nu\delta}^2(p)e^{-\iota\mathbf{q}\cdot\mathbf{R}_{\delta\beta}} \tag{9}$$

and the Bloch factor

$$Y = N^{-3/2}\sum_{\beta=1}^N e^{\iota(k-g)g\beta a} = \frac{\tau}{N^{3/2}}\sum_G \delta(k - g + G),$$

$$g = q\cos\theta, \tag{10}$$

which reflects the conservation of electron momentum along the molecular axis

$$q\cos\theta = k + G. \tag{11}$$

Here, θ is the angle between the chain axis and the Auger electron momentum $\mathbf{q}$; $G = 2\pi j/a$ with $j = \pm 1, \pm 2, \ldots, \pm N$ is the reciprocal lattice vector. The index δ is omitted in Eq. (9) because the Coulomb integral is a one-center integral. The Eq. (11) expresses momentum conservation of the total participator Auger scattering process: The sum of the Auger electron momentum ($q \cos \theta$), the momentum of the valence hole ($-k$) and the lattice momentum G in the final state vanishes because the total momentum in the initial state is zero. Only the photon momentum is neglected in this expression.

Averaging over all randomly-oriented PPV molecules in the sample, conservation of momentum according to Eq. (10) yields the following expression for the RPE cross section:

$$\sigma(E, \omega) = \frac{Nd^2}{q\tau^2} \sum_{n,G} \int_0^{\pi/a} dk |\mathcal{F}_k|^2$$
$$\times \rho \, \delta(\omega - E - (\epsilon_n - \epsilon_0) + E_{ik}), \quad (12)$$

where

$$\rho = \frac{1}{2}[1 + (\mathbf{e} \cdot \hat{\mathbf{d}})^2 + [1 - 3(\mathbf{e} \cdot \hat{\mathbf{d}})^2] \cos^2 \theta],$$

$$\cos \theta = \frac{k + G}{q} \quad (13)$$

is the polarization factor. This factor takes accounts for the angle between the electric field vector of the light and the axis of the individual chains. Here $\hat{\mathbf{d}} = \mathbf{d}/d$ and $|k + G|/q < 1$. Because in the experiment $q \approx 4.5$ a.u.$^{-1}$ is much larger than $k \sim \pi/a \approx 0.24$ a.u.$^{-1}$, the polarization function ρ [given in Eq. (13)] depends only very weakly on k.

This discussion leads us to conclude that momentum conservation (11) does *not introduce any special correlation between the momenta of electrons* in the unoccupied (p) and occupied (k) bands in the participator Auger scattering process. Clearly the experimental observations regarding the dispersion of the π_3- and π_4-RPE peaks can not be explained by the character of the electronic matrix elements alone. Vibrational degrees of freedom need to be considered.

B. Lifetime vibrational interference

Much previous work on lifetime vibrational interference (LVI) focussed on free molecules with few degrees of vibrational freedom. In these relatively simple systems vibrational sublevels are well resolved. This is not the case in most polyatomic molecules and solids. Quite often an unresolved vibrational peak profile closely resembles that of a single effective mode[44] and can be described by a single Gaussian peak. Such a one-mode approximation is widely used in describing x-ray and electron emission spectra and will be used here as well.

The overall dispersion of the RPE peaks[20] can be strongly distorted by LVI.[45] Moreover, the dispersion can be different depending on the electronic states involved. This has been confirmed by many experiments on small free molecules[21] and molecular solids.[46,47]

The LVI effect has its origin in the overlap between the vibrational densities of states in the ground, intermediate and final states of the scattering process. The first step, x-ray absorption, depends on the Franck-Condon (FC) amplitudes $\langle m|0 \rangle$. These amplitudes are maximal for vertical transitions. To illustrate this fact, we consider large vibrational quantum numbers m with vibrational energies $\epsilon_m = \epsilon_V$. In this case the FC amplitudes describe a Gaussian profile[44,48]

$$\langle m|0 \rangle \approx D_{m0}(\epsilon_m) = \frac{1}{\pi^{1/4}\sqrt{\Delta_1}} \exp\left(-\frac{(\epsilon_m - \epsilon_V)^2}{2\Delta_1^2} \right),$$

$$m \gg 1. \quad (14)$$

The effective width of this function, $\Delta_1 = F_c a_0$, is defined by the slope of the potential of the core-excited state, $F_c = |dU_c/dR|_0$, at the equilibrium geometry and the amplitude of vibrations, $a_0 = 1/\sqrt{M\omega_0}$. Here ω_0 and M are the frequency of the vibrational mode and the effective nuclear mass corresponding to this mode, respectively. The scattering amplitude as given in Eq. (3) is maximal when two conditions are fulfilled: the FC amplitude $\langle m|0 \rangle$ must be large and the resonant denominator small.

The FC amplitude of the decay step can be approximated by a Gaussian function as well

$$\langle n|m \rangle \approx D_{nm}(\epsilon_n - \epsilon_m) = \frac{1}{\pi^{1/4}\sqrt{\Delta_2}} \exp\left(-\frac{(\epsilon_n - \epsilon_V' - \epsilon_m)^2}{2\Delta_2^2} \right). \quad (15)$$

The position of the maximum of this FC distribution is called ϵ_V'. This simplified model is self-consistent because it obeys an important rule of the LVI theory—closure: $\Sigma_m \langle n|m \rangle \times \langle m|0 \rangle = \langle n|0 \rangle$. Because of the high density of vibrational states in large molecules, the sum over vibrational quantum numbers can also be replaced by an integration:[49,50] $\Sigma_n \approx \int d\epsilon_n/\omega_0$:

$$\sigma(E, \omega) = \frac{Nd^2}{q\tau^2\omega_0} \sum_G \int_0^{\pi/a} dk |\mathcal{F}_k|^2 \rho,$$

$$\epsilon_n = \omega - E + \epsilon_0 + E_{ik},$$

$$\mathcal{F}_k = \frac{1}{\omega_0} \int_0^{\pi/a} dp \int d\epsilon_m \frac{\tilde{Q} D_{nm}(\epsilon_n - \epsilon_m) D_{m0}(\epsilon_m)}{\omega - (E_{\nu p} - E_{1s}) - (\epsilon_m - \epsilon_0) + \iota\Gamma}. \quad (16)$$

Keeping in mind the role of the vibrational density of states in the LVI effect, and the fact that the density of vibrational states in the ground, intermediate and final states is determined by the (electronic) potential surfaces of these states an important feature of LVI in molecular solids should be noted. If the potential surfaces differ strongly from each other a large phonon broadening is expected. The slope of these potential surfaces is formed by the spatial distribution of electron densities in the various states. Thus the phonon broadening could be a fingerprint of transitions between localized or delocalized electronic states.

V. NUMERICAL SIMULATIONS

Two scattering channels, $|0\rangle \rightarrow |1s^{-1}\pi_6^*\rangle \rightarrow |\pi_3^{-1}\psi_{\mathbf{q}}\rangle$ and $|0\rangle \rightarrow |1s^{-1}\pi_5^*\rangle \rightarrow |\pi_4^{-1}\psi_{\mathbf{q}}\rangle$, form the RPE profile

$$\sigma(E,\omega) = \sigma_{\pi_3}(E,\omega) + \zeta \sigma_{\pi_4}(E,\omega) \tag{17}$$

in the low binding-energy region up to about 4.5 eV. Due to the different nature of the electronic states involved (localized or delocalized), the $\pi_6^* - \pi_3$ and $\pi_5^* - \pi_4$ scattering channels differ qualitatively from each other. Indeed, under excitation from the localized C($1s$) core-level to the localized π_6^*-state the interatomic interaction is not strongly changed in comparison with the excitation to the delocalized π_5^*-band, resulting in a different vibrational broadening for these channels. This motivates the choice of a smaller vibrational broadening Δ_1 for the π_3 than for the π_4-RPE channel [see Eq. (14)]. In the simulations, we used $\Delta_1 = 0.12$ eV and $\Delta_2 = 0.6$ eV for the $\pi_6^* - \pi_3$ and $\Delta_1 = \Delta_2 = 0.6$ eV for the $\pi_5^* - \pi_4$ channel; ϵ_V is assumed to be equal to $\epsilon_{V'}$. A vibrational broadening of $\Delta_2 = 0.6$ eV corresponds approximately to the experimental widths of the π_3- and π_4-peaks in the spectra.

In a first attempt, calculations were performed using k-independent Coulomb matrix elements ($\tilde{Q}_{\pi_3} = 1$, $\zeta \tilde{Q}_{\pi_4} = 0.007$) and the band structure displayed in Fig. 2 for the final state. For the intensity of the π_4 band, a factor $\zeta = 0.007$ was used to provide a better agreement with experiment. From the experiment, the distorted π_5^*-band width is essentially lowered from 2.7 eV to 1.4 eV (see Sec. II). At $k = \pi/a$, the energetic distance between the π_6^*- and π_5^*-bands is taken to be $E_{\pi_6^*} - E_{\pi_5^*} = 0.67$ eV.

Under these conditions, a double-peak structure of $\sigma_{\pi_4}(E,\omega)$ is obtained in the simulated spectrum (see dashed profile in Fig. 7), which represent the two van-Hove singularities in the density of electronic states coming from the two band edges (at $k = 0$ and π/a) of the π_4-band. However, in the experimental RPE spectra (Fig. 4) the π_4-related feature has a high intensity at the low-energy band edge related to the singularity at $k = \pi/a$ while for the singularity at $k = 0$ the intensity is rather weak. This discrepancy can be overcome by making the electronic (Coulomb) matrix elements $\tilde{Q}$ [Eq. (16)] k dependent. This dependence of the lifetime broadening on k is frequently invoked to explain the deviation of the spectral profile from the density of states.[51] It seems that the k dependence of $\tilde{Q}$ is more important. These simulations proof that the deviation of the spectral profile from the density of states in the nonradiative participator-type decay spectra of solids is largely *caused by the dependence of the Coulomb matrix elements on k.*

In the final calculations for the $\pi_5^* - \pi_4$ channel, $\tilde{Q}^2(k)$ has the momentum-dependence depicted in Fig. 6. The use of these k-dependent Coulomb matrix elements is equivalent to an alternative approach of creating an effective band dispersion $E_{\pi_4,k}^{eff}$ for the π_4 band, by maintaining momentum-
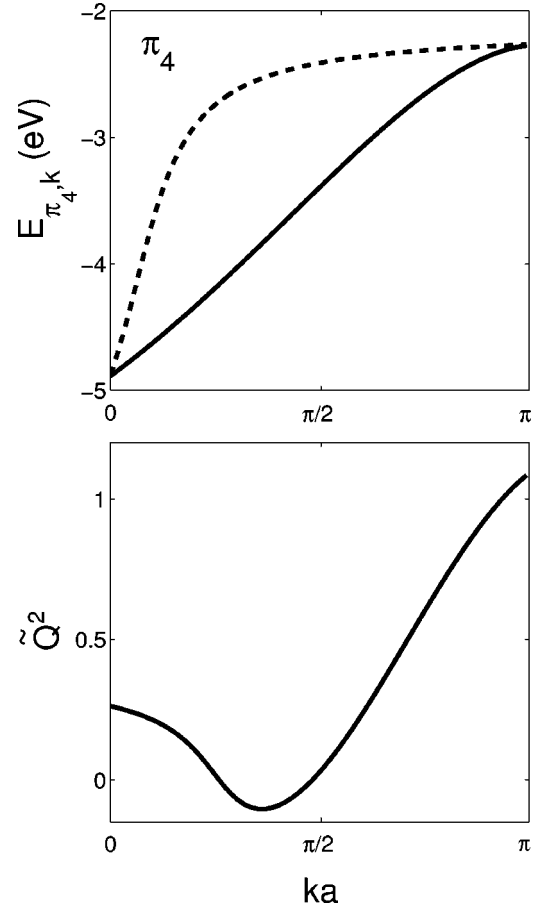

FIG. 6. (a) The energy of the π_4 band, $E_{\pi_4,k}$ (solid line), and of the modified, effective π_4 band, $E_{\pi_4,k}^{eff}$ (dashed line). (b) The square of the decay Coulomb matrix elements $\tilde{Q}^2$ for the π_4 band as a function of the electron momentum k.

independent Coulomb matrix elements. This effective dispersion suppresses the density of states at $k = 0$ and is shown in Fig. 6.

VI. COMPARISON OF THEORETICAL MODEL AND MEASURED SPECTRA

The discussion on momentum conservation in RPE of one-dimensional organic semiconductors essentially ruled out that mechanism as the origin of the dispersion of the localized and delocalized final states. LVI, on the other hand, shows the proper dependence on the localization of the final state wave functions. A comparison with the calculated scattering cross sections is necessary to confirm the origin of the dispersion features. The total computed RPE cross sections [Eq. (17)] are plotted in Fig. 7. These cross sections reproduce the dispersion behavior found in the measured spectra (Fig. 4) for the π_3- and π_4-related final states (Fig. 8). The origin of the different behavior is found in *the magnitude of vibrational broadening for core excitation into localized and delocalized unoccupied bands.* Thus the dispersion of the π_3-related peak depends strongly on the vibrational broadening Δ_1. A doubling of Δ_1 gives worse agreement with experimental spectra (see dashed profile in Fig. 8).
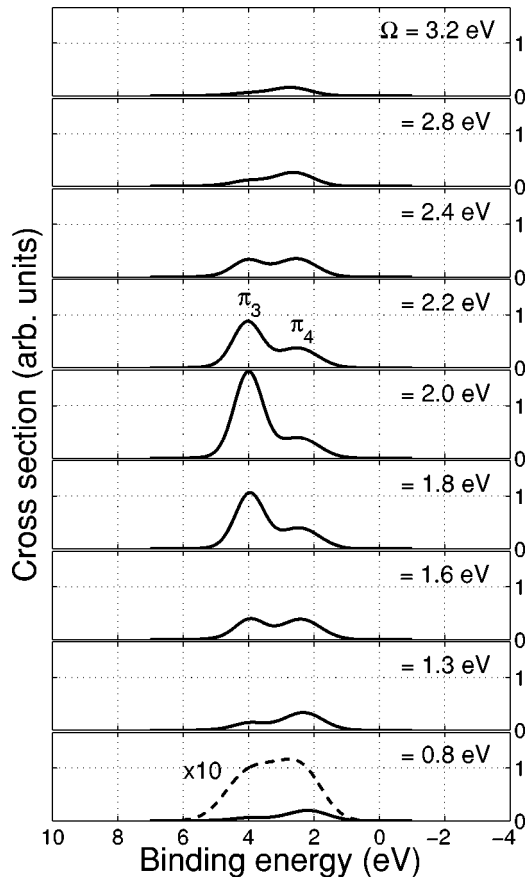
FIG. 7. The evolution of simulated poly(*para*-phenylenevinylene) RPE cross section according to Eq. (17) with the detuning of the photon energy $\Omega = \omega - 283.1$ eV, using $\Gamma = 0.1$ eV, $\Delta_1 = 0.12$ eV and $\Delta_2 = 0.6$ eV for the $\pi_6^* - \pi_3$ scattering channel and $\Delta_1 = \Delta_2 = 0.6$ eV for the $\pi_5^* - \pi_4$ channel and the band dispersion of the effective π_4-band, $E_{\pi_4,k}^{eff}$ (full line). Simulated spectra are plotted relative to the Fermi level. The dashed line shows $\sigma_{\pi_4}(E, \omega)$ for the $\pi_5^* - \pi_4$ channel using the original π_4 band shown in from Fig. 2 and $\tilde{Q} = 1$.
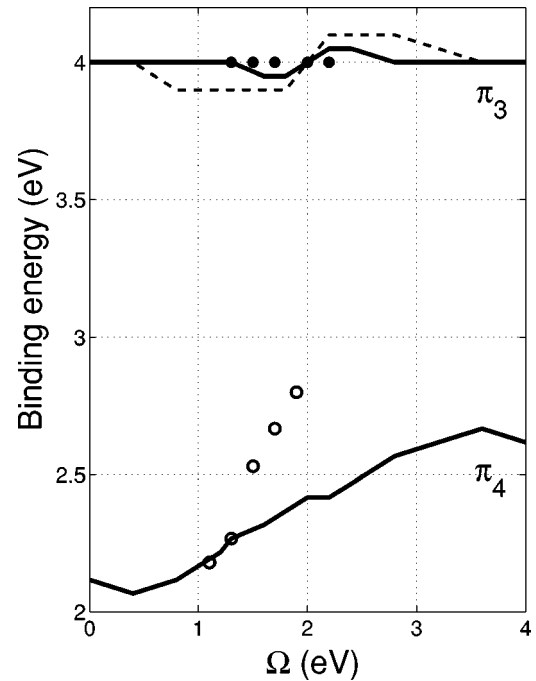

FIG. 8. Experimental (filled and empty circles for the $\pi_6^* - \pi_3$ and $\pi_5^* - \pi_4$ scattering channels, respectively) and simulated (solid lines) peak dispersions in resonant photoelectron emission spectra of PPV as a function of the detuning of the photon energy, $\Omega = \omega - 283.1$ eV. The dashed line shows the peak dispersion for the $\pi_6^* - \pi_3$ channel in the case of $\Delta_1 = 0.24$ eV. Other parameters are the same as in Fig. 7.

VII. SUMMARY

A strong sensitivity of the dispersion of spectral RPE features on the x-ray excitation energy is found experimentally in PPV. The dispersion behavior follows the localization character of the final one-hole states populated in the resonant scattering process. The behavior originates in scattering from a highly localized core-excited electronic state and is motivated by the apparent deviations from linear, Raman dispersion. This behavior arises through the interplay of the degree of electronic localization (expressed as the band width of an electronic state) and vibrational broadening. In other words, electronic localization affects the lifetime vibra-tional interference *via* the (electronic) potential surfaces in the initial, intermediate, and final states. Additionally, evidence is found that in (quasi-one-dimensional) solids, the Coulomb matrix elements exhibit a significant dependence on the momentum k of the electron in the occupied bands which is emitted in the participator decay process. That is, this nonradiative resonant process is sensitive to distinct parts of the Brillouin zone.

*Email address: raifr@ifm.liu.se

†Permanent address: Institute of Automation and Electrometry, 630090 Novosibirsk, Russia.

‡Present address: Swedish LCD Center, Forskargatan 3, Teknik-dalen, 781 70 Borlänge, Sweden.

[1] G. Horrowitz, Adv. Mater. (Weinheim, Ger.) **10**, 365 (1998).

[2] H. Sirringhaus, N. Tessler, and R.H. Friend, Science **280**, 1741 (1998).

[3] J.H. Burroughes, D.D.C. Bradley, A.R. Brown, R.N. Marks, R.H. Friend, P.L. Burn, and A.B. Holmes, Nature (London) **347**, 539

(1990).

[4] W.R. Salaneck, R.H. Friend, and J.L. Brédas, Phys. Rep. **319**, 231 (1999).

[5] C.B. Duke, W.R. Salaneck, T.J. Fabish, J.J. Ritsko, H.R. Thomas, and A. Paton, Phys. Rev. **18**, 5717 (1978).

[6] W.R. Salaneck, C.B. Duke, W. Eberhardt, E.W. Plummer, and H.J. Freund, Phys. Rev. Lett. **45**, 280 (1980).

[7] Z.G. Soos, S. Ramasesha, and D.S. Galvão, Phys. Rev. Lett. **71**, 1609 (1993).

[8] J.L. Brédas, J. Cornil, and A.J. Heeger, Adv. Mater. (Weinheim, Ger.) **8**, 44 (1996).

[9] K. Seki, U.O. Karlsson, R. Engelhardt, E.-E. Koch, and W. Schmidt, Chem. Phys. **91**, 459 (1984).

[10] J. Fink, N. Nücker, B. Scheerer, A. vom Felde, H. Lindenberger, and S. Roth, in *Electronic Properties of Polymers and Related Compounds, Proceedings of an International Winter School Kirchberg II*, edited by H. Kuzmany, M. Mehring, and S. Roth (Springer-Verlag, Heidelberg, 1987), Vol. 76.

[11] M. Knupfer, J. Fink, E. Zojer, G. Leising, U. Scherf, and K. Müllen, Phys. Rev. B **57**, R4202 (1998).

[12] M. Knupfer, T. Pichler, M.S. Golden, J. Fink, M. Murgia, R.H. Michel, R. Zamboni, and C. Taliani, Phys. Rev. Lett. **83**, 1443 (1999).

[13] W.R. Salaneck, S. Stafström, and J.L. Brédas, *Conjugated polymer surfaces and interfaces: Electronic and chemical structure of interfaces for polymer light emitting devices* (Cambridge University Press, Cambridge, 1996).

[14] J. Stöhr, *NEXAFS Spectroscopy*, Springer Series in Surface Science Vol. 25 (Springer, Berlin, 1992).

[15] P.A. Brühwiler, A.J. Maxwell, A. Nielsson, R.L. Whetten, and N. Mårtensson, Chem. Phys. Lett. **193**, 311 (1992).

[16] W. Eberhardt, R. Dudde, M.L.M. Rocco, E.E. Koch, and S. Bernstorff, J. Electron Spectrosc. Relat. Phenom. **51**, 373 (1990).

[17] S. Svensson and A. Ausmees, Appl. Phys. A: Mater. Sci. Process. **65**, 107 (1997).

[18] P. Eisenberger, P.M. Platzman, and H. Winick, Phys. Rev. Lett. **36**, 623 (1976).

[19] F. Gel'mukhanov and H. Ågren, Phys. Rep. **312**, 87 (1999).

[20] F. Gel'mukhanov and H. Ågren, Phys. Rev. A **54**, 3960 (1996).

[21] M.N. Piancastelli, J. Electron Spectrosc. Relat. Phenom. **107**, 1 (2000).

[22] F. Gel'mukhanov, L.N. Mazalov, and N.A. Shklyaeva, Zh. Éksp. Teor. Fiz. **71**, 960 (1976) [Sov. Phys. JETP **44**, 504 (1977)].

[23] F. Gel'mukhanov and H. Ågren, Phys. Rev. A **49**, 4378 (1994).

[24] F. Gel'mukhanov and H. Ågren, Phys. Lett. A **193**, 375 (1994).

[25] S. Aksela, E. Kukk, H. Aksela, and S. Svensson, Phys. Rev. Lett. **74**, 2917 (1995).

[26] L. Braicovich, M. Taguchi, F. Borgatti, G. Ghiringhelli, A. Tagliaferri, N.B. Brookes, T. Uozumi, and A. Kotani, Phys. Rev. B **63**, 245115 (2001).

[27] F. Gel'mukhanov, A. Baev, Y. Luo, and H. Ågren, Chem. Phys. Lett. **346**, 437 (2001).

[28] Z.W. Gortel and D. Menzel, Phys. Rev. B **64**, 115416 (2001).

[29] P.A. Brühwiler, O. Karis, and N. Mårtensson, Rev. Mod. Phys. **74**, 703 (2002).

[30] P.A. Brühwiler, A.J. Maxwell, C. Puglia, A. Nilsson, S. Andersson, and N. Mårtensson, Phys. Rev. Lett. **74**, 614 (1995).

[31] P.A. Brühwiler, A.J. Maxwell, P. Rudolf, C.D. Gutleben, B. Wästberg, and N. Mårtensson, Phys. Rev. Lett. **71**, 3721 (1993).

[32] J. Kikuma and B.P. Tonner, J. Electron Spectrosc. Relat. Phenom. **82**, 41 (1996).

[33] D. Menzel, G. Rocker, H.-P. Steinrück, D. Coulman, P.A. Heimann, W. Huber, P. Zebisch, and D.R. Lloyd, J. Chem. Phys. **96**, 1724 (1991).

[34] P.L. Burn, D.D.C. Bradley, A.R. Brown, R.H. Friend, D.A. Halliday, A.B. Holmes, A. Kraft, and J.H.F. Martens, in *Electronic Properties of Polymers, Proceedings of an International Winter School Kirchberg*, edited by H. Kuzmany, M. Mehring, J. Fink, and S. Roth (Springer-Verlag, Heidelberg, 1992), Vol. 107.

[35] A. Andersson, T. Kugler, M. Lögdlund, A.B. Holmes, X. Li, and W.R. Salaneck, Synth. Met. **106**, 13 (1999).

[36] M. Lögdlund, W.R. Salaneck, F. Meyers, J.L. Brédas, G.A. Arbuckle, R.H. Friend, A.B. Holmes, and G. Froyer, Macromolecules **26**, 3815 (1993).

[37] K. Xing, M. Fahlman, M. Lögdlund, D.A. dos Santos, V. Parenté, R. Lazzaroni, J.L. Brédas, R.W. Gymer, and W.R. Salaneck, Adv. Mater. (Weinheim, Ger.) **8**, 971 (1996).

[38] The base pressure in the UHV system of the endstation of BL I311 is less than 2×10^{-10} mbar, and that of BL 411 less than 1×10^{-9} mbar.

[39] C.D. Duke and W.K. Ford, Int. J. Quantum Chem., Quantum Chem. Symp. **17**, 597 (1983).

[40] J. Obrzut, M.J. Obrzut, and F.E. Karasz, Synth. Met. **29**, E109 (1989).

[41] E. Ettedgui, H. Razafitrimo, Y. Gao, B.R. Hsieh, and M.W. Ruckman, Synth. Met. **78**, 247 (1996).

[42] A. Rajagopal, M. Keil, H. Sotobayashi, A.M. Bradshaw, M.A. Kakimoto, and Y. Imai, Langmuir **13**, 5914 (1997).

[43] The definition of $\mathbf{R}_\beta$ is not unique because one can put this "center" in any place of the unit cell. However, such a shift of $\mathbf{R}_\beta \rightarrow \mathbf{R}_\beta + a$ results only in a phase factor $\exp(\iota pa)$ of the wave function. This phase factor can be omitted.

[44] H. Köppel, W. Domcke, and L.S. Cederbaum, Adv. Chem. Phys. **57**, 59 (1984).

[45] F. Gel'mukhanov, L. Mazalov, and A. Kondratenko, Chem. Phys. Lett. **46**, 133 (1977).

[46] A.B. Preobrajenski, A.S. Vinogradov, S.L. Molodtsov, S.K. Krasnikov, T. Chassé, R. Szargan, and C. Laubschat, Phys. Rev. B **65**, 205116 (2002).

[47] A.B. Preobrajenski, A.S. Vinogradov, S.L. Molodtsov, S.K. Krasnikov, T. Chassé, R. Szargan, and C. Laubschat, Chem. Phys. Lett. **368**, 125 (2003).

[48] J.W. Gadzuk, Phys. Rev. B **20**, 515 (1979).

[49] O. Plashkevych, H. Ågren, V. Carravetta, G. Contini, and G. Polzonetti, Chem. Phys. Lett. **327**, 7 (2000).

[50] T. Privalov, O. Plashkevych, F. Gel'mukhanov, and H. Ågren, J. Chem. Phys. **113**, 3734 (2000).

[51] S. Eisebitt, Ph.D. thesis, Universität Köln, 1996.